A Vacuum-driven Origami "Magic-ball" Soft Gripper

Shuguang Li[1,2], John J. Stampfli[2], Helen J. Xu[2], Elian Malkin[2], Evelin Villegas Diaz[1,3], Daniela Rus[2] and Robert J. Wood[1]

***Abstract*— Soft robotics has yielded numerous examples of soft grippers that utilize compliance to achieve impressive grasping performances with great simplicity, adaptability, and robustness. Designing soft grippers with substantial grasping strength while remaining compliant and gentle is one of the most important challenges in this field. In this paper, we present a light-weight, vacuum-driven soft robotic gripper made of an origami "magic-ball" and a flexible thin membrane. We also describe the design and fabrication method to rapidly manufacture the gripper with different combinations of low-cost materials for diverse applications. Grasping experiments demonstrate that our gripper can lift a large variety of objects, including delicate foods, heavy bottles, and other miscellaneous items. The grasp force on 3D-printed objects is also characterized through mechanical load tests. The results reveal that our soft gripper can produce significant grasp force on various shapes using negative pneumatic pressure (vacuum). This new gripper holds the potential for many practical applications that require safe, strong, and simple grasping.**

I. INTRODUCTION

Soft-bodied robots can offer safer and more compliant interactions between machines, the environment, and humans, as compared to traditional rigid (and often powerful and dangerous) robots [1]–[4]. In addition to safe interactions, their flexibility can provide soft robots with other useful properties, such as adaptability and robustness. Specific to manipulation, the lack of rigid elements allows soft grippers to conform to objects with both newfound ease and high grasping performance [5], [6].

Traditional rigid robotic grippers are designed to precisely perform manipulation tasks, and they often require precise measurements of the target object's location and geometry prior to grasping [7]. Thus, their ability to grasp different objects and to handle uncertainty are limited. To overcome these limitations, there has been significant progress in the development of soft grippers in recent years. Numerous materials and actuation methods have been used to build soft grippers, such as grippers made from electroactive polymers [8], electrostatic grippers [9], [10], magnetorheological fluid-based grippers [11], [12], underactuated compliant grippers [13]–[15], auxetic-structure-based grippers [16], [17], and pneumatically-driven elastomer or rubber grippers [18]–[25].

Among these different approaches, pneumatically-driven soft grippers are still the most popular due to their simplicity, high-performance, and low-cost. Most pneumatic soft grippers are designed with an anthropomorphic morphology, and they are usually powered by compressed air. These soft-finger grippers can successfully grasp various objects, including soft and delicate objects [18], [19]. However, the grasp force for this class of gripper is greatly limited by the strength of the soft-finger structures and safety limitations of the applied positive pressure. Another popular design for pneumatically-driven soft grippers is the ball-shaped gripper based on granular jamming [26], [27]. This soft gripper can be powered by negative air pressure (vacuum), and has the ability to grasp a wide range of objects. However, the grasping postures are very limited, due to the required preloading force. Nevertheless, the jamming gripper demostrates that even a vacuum-driven soft robot can produce sufficient forces for reliable grasping. Furthermore, recent studies also demonstrate that vacuum-driven soft actuators can produce a wide variety of powerful motions [28]–[30].

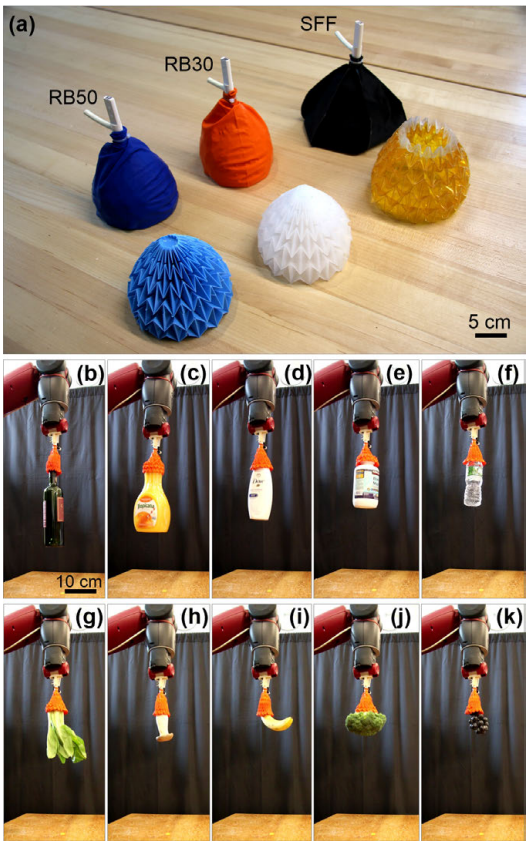

Fig. 1: (a) Three diverse origami "magic-ball" soft grippers with their respective skeletons. A robot with the "magic-ball" gripper (RB30) picks up various objects: (b)-(f) bottles; and (g)-(k) foods.

[1]John A. Paulson School of Engineering and Applied Sciences, and the Wyss Institute for Biologically Inspired Engineering, Harvard University, Cambridge, MA 02138, USA
[2]Computer Science and Artificial Intelligence Laboratory, Massachusetts Institute of Technology, Cambridge, MA 02139, USA
[3]St. Mary's University, San Antonio, TX 78228, USA
lisg@seas.harvard.edu; rus@csail.mit.edu; rjwood@seas.harvard.edu

In this paper, we propose a new design for a vacuum-driven soft gripper that has a hollow hemispherical body shape. This soft gripper can envelope an entire object, or part of a target object, for grasping and manipulation (Fig.1). The results from our study reveal that the soft gripper is able to grasp a large variety of different objects (including 12 food items, 19 different bottles and cups, and 14 miscellaneous items), and also demonstrate sufficient robustness (allowing up to 40% axial offset in grasping) and a large grasp force (holding loads up to 120 N at -60 kPa – more than 120 times the gripper's weight).

This paper highlights the following contributions: (1) a simple soft gripper architecture consisting of an origami "magic-ball" skeleton and a flexible thin membrane; (2) two distinct fabrication approaches for the origami skeleton and two different choices of low-cost membrane materials; and (3) performance characterization of the gripper using both a collection of everyday objects and a set of test objects with various geometries.

II. Design and Fabrication

A. The working principle and design of the gripper

The origami "magic-ball" is a well-established origami design. It is folded from a rectangular piece of paper pre-creased with a repeating waterbomb pattern that is offset by a half-unit on every new row. The waterbomb pattern features a square with folds along its diagonals and a vertical axis of radial symmetry. This "magic-ball" structure can be reversibly changed between a spherical shape and a cylindrical shape, therefore it has been utilized previously in the development of morphing robots [31]–[36].

We build on our previous research that introduced the concept of Fluid-driven Origami-inspired Artificial Muscle (FOAM) [30]. FOAM consists of an airtight skin enclosing a foldable skeleton and a fluid medium. This type of artificial muscle contracts under negative pressure (i.e., when the external pressure exceeds the pressure inside the skin). The skin constricts the skeleton and forces compression along fold lines once the fluid is drawn out such that the kinematics of the actuator are controlled by the folding of the skeleton.

The origami "magic-ball" can exhibit a significant radial contraction with a volume reduction of more than 90% [30]. Furthermore, if one end of the origami "magic-ball" is fixed and closed, then the other end can be opened to form a hollow hemispherical shape (Fig.2). This particular configuration of the origami "magic-ball" is suitable as the basis for the skeleton of a gripper for enveloping grasps based on the working principle of FOAM [30]. A high-strength and compliant grasping motion can be achieved by applying a vacuum into this system when the skeleton is enclosed in an airtight membrane (skin). The basic working principle of our gripper is explained in Fig.2 (a), and a prototype is shown in Fig.2 (c) and (d) from different perspectives. The geometry of the "magic-ball" skeleton for our gripper is presented in Fig.2 (b). A commonly accepted starting dimension is a 16 $\times$ 8 grid of waterbomb unit square folds, with each square side length of 30 mm. Restricting the upper radius to 20 mm accommodates a space-efficient and robust connection between the structural origami-based component and the rest of the gripper. A height of five vertical units is used in the final gripper design to create the largest attainable lower radius to effectively grip objects.

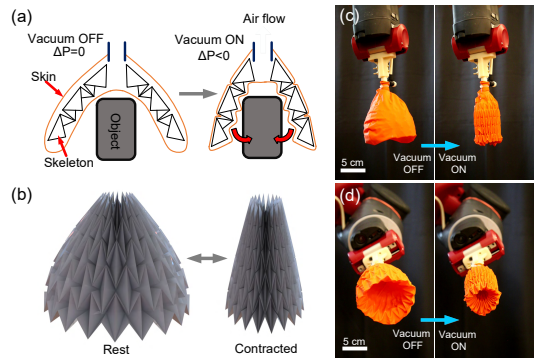

Fig. 2: (a) The working principle of our gripper; (b) origami "magic-ball" skeleton; and a prototype of our gripper from different perspectives (c)-(d).

B. Fabrication of the gripper

The grippers are comprised of three fundamental portions: the origami-based skeleton structure, the airtight skin to encase the structure, and the connector that allows the gripper to be attached as an end-effector on a manipulator.

1) Skeleton: Creating the origami-based structure through casting and self-folding methods allowed for increased durability, precision, and efficiency, beyond those of just manual folding methods.

a) Casting of silicone rubber skeleton: The casting method was pursued for the durability provided by a structure made of silicone rubber. The mold pieces were formed around the Solidworks "magic-ball" model (Fig.2 (b)) and 3D-printed using an FDM printer (Stratasys Fortus 400) with ABS materials (shown in Fig.3). The interlocking geometry of the core and the cavity required the latter to be split into 16 components such that each individual piece around the core could freely slide out of its position. The handles on the sides of the cavity pieces allow them to be securely bolted together for molding. In order to combat air bubbles being trapped in the upward-pointing vertices of the waterbomb units, 1 mm diameter venting holes were drilled to connect these vertices to the exterior of the cavity. The mold rubbers used are Smooth On's Dragon Skin 30 (Shore hardness of 30A) and Smooth Sil 950 (Shore hardness of 50A) which were poured through a 20 mm opening at the topmost point of the cavity and cured over 16 and 18 hours respectively.

b) Self-folding of plastic skeleton: Following prior examples of self-folding origami in our previous work [37]–[39], the fabrication of the self-folding "magic-ball" based origami involves a layer of shape memory polymer (SMP) adhered between two layers of laser-cut structural material. The structural material of 0.11 mm thick polyethylene terephthalate (PET) was cut such that each valley fold would have a gap of 2.5 mm and each mountain fold would be cut through. In addition, there were holes at every corner to reduce tear at the points of peak stress in the design.

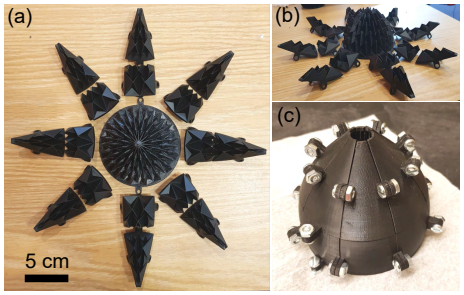

Fig. 3: 3D-printed molds for casting the "magic-ball" skeletons with silicone rubbers

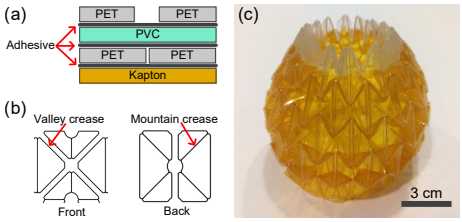

Fig. 4: (a) The laminated composites for our self-folding "magic-ball"; (b) the complementary laser-cutting patterns for both sides of a waterbomb unit square; and (c) a self-folded "magic-ball" skeleton.

At each intersection where two edges meet, the pieces were also rounded to as to eliminate sharp corners. The sheets of PET were cut using a laser cutter (Universal Laser Systems, Inc.) to the patterns shown in Fig.4 (b). The self-folding magic ball was made with heat-shrink PVC plastic as the SMP layer and high temperature adhesive (McMaster-Carr High Temperature Glue-on-a-roll) to bond the PET structural layers to the PVC. Before the heat-activated folding, high temperature Kapton tape was adhered to the sheet such that the two edges were merged so the 2D shape became a 3D cylinder. In order to add strength to each hinge fold such that the strength was beyond that of just shrunken PVC film, a Kapton sheet was adhered to the entire inside of the cylinder with the exception of the top half of the top-most square layer. The lamination structure of the self-folding composite structure is shown in Fig.4 (a). The cylinder was then folded in a oven for 30 seconds at 100 degrees celsius (see the self-folded "magic-ball" in Fig.4 (c)). The lack of Kapton on the uppermost half-layer of unit squares allowed urethane glue (3M 3535 Fast-Hardening Urethane) to stick the top layer of unit squares together after 30 minutes of curing.

2) Skin:

a) Latex-rubber-balloon skin: Of the airtight possibilities to encase the structural portion of the gripper, 27-inch latex-rubber balloon offered a simple solution. The use of a balloon enabled the gripper skin to be easily replaced. The elastic deformation capability of a balloon also allows the skin to closely conform to the origami skeleton. This conformity allows the teeth-like corners of unit square hinges to acquire a firm grip on the target object from all sides as shown in Fig.2 (d).

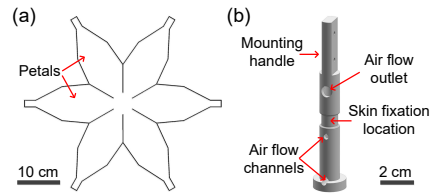

Fig. 5: (a) Laser-cutting patterns for the fabric skin; and (b) CAD model of the connector.

b) Airtight fabric skin: Another possibility for a gripper skin is a TPU-coated nylon fabric sheet. This material could be cut into a flower shape (as shown in Fig.5 (a)), and the edges of the petals could be sealed by an impulse heat sealer (AIE-410FL, American International Electric, Inc.) such that it maintained the shape of the gripper (as shown in Fig.1 (a)).

3) Connector: The connector was designed to provide a mechanical connection between the gripper and an external mount, and to create a pneumatic connection to the inside of the gripper. As shown in Fig.5 (b), the base has a diameter of 18 mm and a height of 5 mm, in order to fit inside of the skeleton without allowing the connector to pull through the skeleton. The neck of the connector is 9 cm tall, and has four holes above where the origami-based structure would sit and four channels at its base to allow airflow both underneath and above the origami-based structure.

4) Assembly: The final assembly of the origami-based structure, skin, and connector involved making sure that the skin was airtight and did not constrain the shape of the structural component. Once the structure was attached to the connector, two Velcro discs were glued to the bottom of the connector and the inside of the corresponding skins using Loctite 401. The skin was then attached to the base of the connector so that it would not fall out from inside the gripper. The end of the skin was fixed to the circular indent in the connector by a zip tie, with rubber tubing underneath to act as a washer and maintain an airtight seal.

5) Three different prototypes: Three different combinations of grippers were created as shown in Fig.1 (a): the self-folded skeleton with fabric skin, denoted as SFF, the rubber molded skeleton of Shore hardness 30 with balloon skin, denoted as RB30, and the rubber molded skeleton of Shore hardness 50, denoted as RB50. For SFF, the structure at the top was glued together around a connector, whereas, for RB30 and RB50, holes were drilled in the top so that the connector could be pushed through. The balloon skin was simply stretched over to fit around the structure, while the fabric skin needed to be sealed around the structure at the edges of the individual petals. A summary of information of these three grippers can be found in Table I. We should note that the proposed gripper structure is scalable. However, it would be challenging to build a gripper at small scales (e.g., maximum diameter <1 cm) using the current fabrication

TABLE I: Summary of the three different grippers

Gripper	Skeleton	Skin	Weight (g)	Dimension (cm) height $\times$ max. diameter	Peak holding force at -60 kPa (4cm-stage-shaped object)
SFF	PET-PVC-Kapton composites	TPU-coated nylon fabric	54	14×11	$\approx$ 30 N
RB30	Silicone rubber (Dragon Skin 30)	Latex rubber balloon	97	13.5×10	$\approx$ 120 N
RB50	Silicone rubber (Smooth-Sil 950)	Latex rubber balloon	105	13.5×10	$\approx$ 80 N

methods.

III. Characterization of the Gripper

A. Object gripping capability

Using a Baxter robot, the RB30 gripper was tested to demonstrate its capability of picking up daily objects. Our gripper is particularly well-suited for picking up bottle-shaped objects because of their thin, vertical form factor, as well as soft and delicate objects owing to the gripper's conforming skeleton. The gripper was able to pick up and hold a variety of foods while being gentle enough to avoid causing damage. It also reliably lifted a range of bottles with weights reaching nearly 2 kg. We should note that the target object's surface condition (e.g., friction) is also an important factor in evaluating the gripper's capability. The maximum diameter of the object grasped and lifted by the gripper was 7 cm (see Fig.6(a)), which is approximately 70% of the gripper's diameter (10 cm). Table II lists all the objects that were successfully grasped by our RB30 gripper in the tests.

In addition, the gripper has sufficient grasping robustness - it can work without perfect axial alignment (allowing up to 40% axial offset) and even when the edge inadvertently folds upwards into the gripper rather than fitting around the object (see the object picking tests with misalignment in Fig.6). This property is particularly useful for picking up miscellaneous objects. Even when the target object's contours fit poorly inside the grasping radius of the gripper, the gripper's ability to conform to irregular shapes allows it to grasp unique objects.

B. Gripping/holding force

The gripping and holding forces were obtained using a universal load test machine (Instron 5544A). We used an extension method, with the machine extending at a rate of 1 mm/s to a final extension of 80 mm. The object to be gripped was lowered into the gripper until there was enough contact to produce a negative 1 N force. A set of objects with different geometries were fabricated using a FDM 3D printer (see Fig.7). The test objects were fixed on the Instron during all the tests, thus their weights did not affect the test results. The first test done was a varying pressure test, and the second was a geometry test, done to compare the ability of the grippers to grasp different shapes of varying sizes. The pressure tests were done seven times for each experimental set-up, and the geometry tests were performed four times for each shape.

The origami gripper was clamped into the Instron machine for gripping and holding force tests. The pressure tests were done by applying a vacuum of -20, -40, -60, and -80 kPa

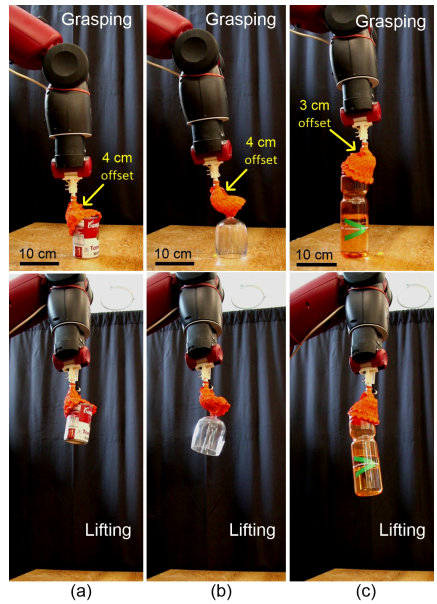

Fig. 6: Axial misalignment of the gripper did not reduce capability of grasping and lifting objects: (a) soup can; (b) wine glass; and (c) water bottle.

for three different grippers. The three grippers tested were the self-folded skeleton with a fabric skin (SFF), the molded skeleton with a shore hardness of 30 with a balloon skin (RB30), and the molded skeleton with a shore hardness of 50 with a balloon skin (RB50). In order to directly compare the relationship between pressure and gripping/holding force, all of the pressure tests were done using a cylinder with a diameter of 4 cm. It was found that there was a direct relationship between pressure and load for each of the three grippers. That is, holding force increased with an increase of pressure (Fig.8 (a)). We found that the RB50 gripper's holding force decreased at -80 kPa. This is probably caused by a pushing force induced by the buckled skeleton of the gripper. Another finding from the plot was that the structure of the gripper and the progression of the object being pulled from it can be clearly seen. In each run of the pressure experiments, there are three very clear drops in load measured (Fig.8 (b)). These three drops correspond to the rows of teeth in our gripper, an identifying part of the origami magic ball structure. Each object began in the third row of teeth in the gripper, so this is consistent with the gripper's structure.

Between the three skeletons, we thought that a more rigid skeleton would provide a much stronger grasp. Instead we found that the SFF gripper did not meet our gripping ability expectations. We determined this unexpectedly weaker grasp to be due in part to the fabric skin of the SFF gripper. The

TABLE II: Objects that successfully grasped by our gripper

Category	Items (weight,gram)
Foods	Broccoli (406), Eggplant (136), Orange (152), Grapes (163), Mushroom (89), Pear (234), Kiwi (76), Potato (309), Bok choy (144), Apple (143), Banana (165), Tomato (114).
Bottles	Soft scrub bleach (1107), Tropicana orange juice (1911), Tomato soup (351), Wine glass (132), Coke can (370), Half-filled water (463), Voss water (552), Izze bottle (556), Wine bottle (636), Simplex (575), Sobe elixir (664), Dove body wash (127), CVS mineral oil (529), Biotherm homme (55), Tide detergent (45), Sprayon release agent (407), Kirkland vitamins (281), Poland Spring bottle water (528), Coke bottle (645).
Misc. Objects	PlayStation controller (180), Soft foam football toy (99), Shoe brush (96), Electric drill (655), Wood plank (133), Hammer (667), Dragon plush (37), Computer mouse (68), Tuna can (174), Rubber duck (51), Flashlight (458), Screwdriver (119), Board marker (27), Shoe (278).

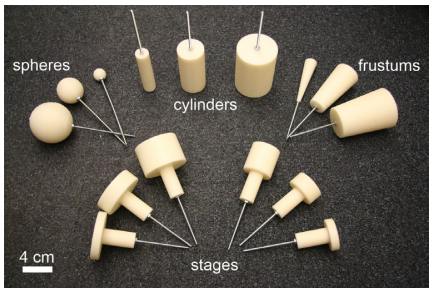

Fig. 7: 3D-printed testing objects with various geometries.

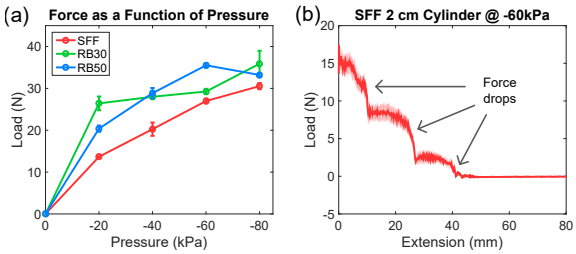

Fig. 8: (a) The holding forces increase with an increase in vacuum pressure. (b) Force drops caused by the teeth slipping of the gripper during extension.

fabric material is very smooth and does not provide much grasping ability, allowing objects to slip more easily. This was not the case for the rubber grippers because the balloon skin was much better at preventing objects from slipping. Although the fabric skin was not optimal for the greatest load, it was much more durable than the balloon skins. Many holes were found in the balloon skin after testing and the skins needed to be replaced, whereas the fabric skin did not get punctured by the skeleton or objects, and did not need to be replaced. Our tests show that different combinations of skeleton and skin can create grippers that excel at particular tasks. Durable skins can be used to grip objects with sharp edges, and more fragile skins can be used for soft objects. We also saw that different skeletons had different profiles. Some of the skeletons had negative readings for the load at certain extensions. Because of the structure of the origami magic ball, at particular extensions some of the skeletons were pushing the objects outward. This occurred more with the more rigid skeletons. For example, the SFF gripper holding the 4 cm cylinder reached an initial negative load (pushing force) of -19 N with a vacuum of -60 kPa (Fig.9 (a)).

The object's geometry tests were performed on the SFF gripper, using 18 different shapes (Fig.7). Each test was done with an applied vacuum of -60 kPa. We tested the gripper using cylinders, spheres, frustums, and "stage" shapes of varying diameter: 2 cm, 4 cm, and 6 cm. Using a variety of geometries allowed us to test the ability of the gripper to grasp a large range of objects, and to determine which shapes the gripper is best at handling. Objects that fit in the second and third row of teeth were grasped much better than those which only fit into the outermost row. The four basic shapes we used for initial geometry tests were a cylinder, sphere, and both the top and bottom parts of a frustum (Fig.9 (a)). All of the 4 cm diameter shapes consistently show two peaks/drops, corresponding to the two rows of teeth that these shapes fit into. The various geometries lead

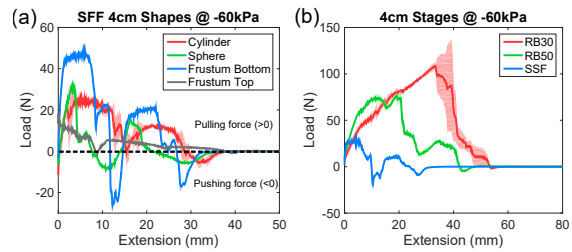

Fig. 9: Holding force comparison of (a) the SFF gripper on objects with different geometries at -60kPa; and (b) the three different grippers on a stage-shaped object (diameter: 4 cm, height: 1 cm) at -60 kPa.

to peak forces at roughly the same extensions, with the first peak occurring at approximately 5 mm. The magnitude of the gripping force, as well as that of the pushing force that occurs, varies depending on the shape itself and the diameter of the shape.

Fig.10 (a) shows how the SFF gripper holds cylinders of various diameters. For this particular shape, the greatest holding force is achieved with the 4 cm diameter, with a peak force of approximately 38 N, while the smaller and larger diameters are not grasped as well. Each diameter was chosen to fit into the gripper's teeth at different rows; the smallest diameter can be grasped by three rows, the middle diameter by two rows, and the largest diameter by just the one row. The plot reflects this, with significant drops where an object slips from a row of teeth. The number of drops in a plot shows how many rows of teeth the object had been gripped by. There is also a considerably large pushing force at several extensions for the cylinders. The initial pushing force for both the 4 cm and 6 cm diameters implies that the cylinders were between rows and were being pushed outward by an inner row further inside the gripper. Different locations within the gripper are better suited to gripping, and these locations are dependent on the diameter and geometry of the shape.

Fig.10 (b) represents the performance of the SFF gripper while holding spheres of varying diameter. The peak force is again achieved with the 4 cm diameter, reaching approximately 32 N. The pushing force is observed to a greater extent than usual for the 6 cm diameter sphere. This is due to the geometry of the shape which prevents the gripper from ever being able to grasp the object. The inner rows have a smaller diameter than the sphere and so the object is expelled outward. For the 2 cm and 4 cm diameter spheres, the data is consistent with the structure of the gripper: these plots for these objects display three drops and two drops, respectively.

Fig.10 (c) represents the gripper holding frustums of different diameters from the top portions (the slimmer ends). This shape is not ideal for gripping, as the geometry enables slipping and favors the pushing force over being grasped. The smallest frustum, with a 2 cm base, was too small to be grasped sufficiently and so the load for this object is very close to 0 N. Once again the peak force was achieved with the 4 cm diameter object, with the gripper consistently reaching the largest holding force with this diameter. The initial peak force for the 4 cm frustum, held from the top,

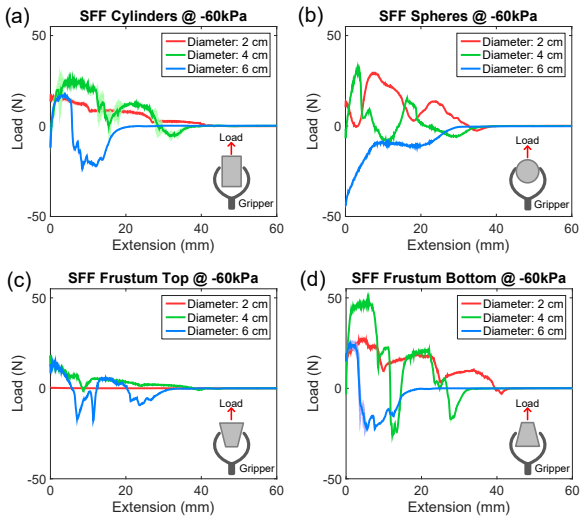

Fig. 10: Holding force comparison of the SFF gripper on different shapes with varying diameters: (a) cylindrical objects; (b) spherical objects; (c) frustum objects from the top portions (the slimmer ends); and (d) frustum objects from the bottom portions (the wider ends). The driven-pressure was at -60 kPa for the tests.

was approximately 18 N.

Trying to grip frustums from the top is not ideal for our gripper, but gripping frustums from the bases (the wider ends) leads to a much greater holding force. The plot of varying diameter of frustums being gripped from the bottom displays that of the four basic shapes we experimented with, this shape is the best for being gripped (Fig.10 (d)). The drops in gripping force can be observed here as well, corresponding to the locations where the gripped object slips between rows of teeth. The peak holding force achieved with this shape was approximately 50 N, and was again reached by gripping the 4 cm diameter object. A shape with the largest diameter being in the innermost portion of the gripper and then decreasing in diameter is an ideal shape for our gripper. This shape, when grasped, forms a mechanical lock that allows the gripper to hold with a much greater force than it does with other objects of the same diameter.

Based on the mechanical lock concept, a stage shape was believed to be an optimal shape for the gripper. The stage shapes used were short cylinders of varying height and diameter, the idea being that the objects could be fully enveloped by the gripper to maximize holding force and form a mechanical lock. First, the SFF gripper was tested at -60 kPa using the different stage shapes in order to determine which stage was best for gripping. Fig.11 (a) and Fig.11 (b) reveal that the 4 cm stage with a height of 1 cm was the best object to grip, although the SFF gripper was unable to perform very well with these objects due to the rigidity of the skeleton. Next, all three grippers were tested at -60 kPa using the 4 cm diameter, 1 cm height stage. Fig.9 (b) shows the different gripping abilities of the grippers. Here, the RB30 gripper greatly outperforms the other grippers with this particular geometry (peak force: 120 N). This can be attributed to the softer skeleton of the RB30 gripper. This softness allows the gripper to conform to the shape of the stage and fully envelope it much more than the more rigid

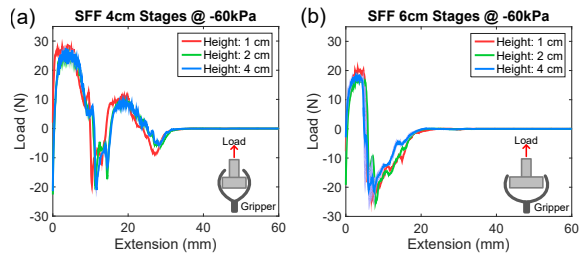

Fig. 11: Holding force comparison of the SFF gripper on (a) stage-shaped objects (diameter: 4 cm) with varying heights; (b) stage-shaped objects (diameter: 6 cm) with varying heights.

SFF and RB50 grippers.

IV. CONCLUSIONS

While soft-bodied robotic grippers are able to grasp a large variety of objects with simple controls, developing a soft gripper with both a compliant structure and sufficient gripping force for object manipulation remains a challenge. In this paper, we proposed a new design for a vacuum-driven origami-based soft gripper. A compliant origami "magic-ball" structure is used as the gripper's internal skeleton, and it is covered by a rubber balloon or a thin fabric sheet. The design details and fabrication process of the gripper are presented in this paper with a recommended combination of material choices for different applications. We demonstrated the capability of our soft grippers by conducting a group of grasping tests on a large collection of daily objects, including foods, bottles, and other miscellaneous items. The gripper's grasp force has also been characterized in this study through mechanical load measurements over a set of 3D printed objects. The results indicate that our soft gripper can grasp a wide range of objects robustly, even at high loading.

Questions remain regarding which materials would optimize the strength, rigidity, and durability of the gripper. Similarly, varying other shapes and dimensions from the original model explored could improve performance for a wider variety of objects or a certain category of objects. It is also possible to modify the gripper's origami skeleton to exert contact forces on an object at desired directions. In our future work, force feedback could be attained for a deeper understanding of the grasping by embedding force and pressure sensors inside the gripper [19], [40], [41]. The addition of different materials to the skin, such as anti-slip tape or gecko-inspired adhesives [42], could increase friction and grasp force on the target objects. Incorporating suction cups into the future gripper design could potentially address the current gripper's limitation of picking up thin and large objects. Additionally, we need to determine the best angle to approach target objects with the origami gripper [43], [44].

ACKNOWLEDGMENT

The authors thank Lillian Chin, John Amend, Daniel Vogt, Jessica Yen, and John Whitehead for their help and suggestions on this work. This material is based on work supported by the Defense Advanced Research Projects Agency (award number: FA8650-15-C-7548), the National Science Foundation (award number: 1830901), JD.com, and the Wyss Institute for Biologically Inspired Engineering.

REFERENCES

[1] D. Rus and M. T. Tolley, "Design, fabrication and control of soft robots," *Nature*, vol. 521, no. 7553, pp. 467–475, 2015.

[2] C. Laschi, B. Mazzolai, and M. Cianchetti, "Soft robotics: Technologies and systems pushing the boundaries of robot abilities," *Sci. Robot.*, vol. 1, no. 1, p. eaah3690, 2016.

[3] G. M. Whitesides, "Soft robotics," *Angewandte Chemie International Edition*, vol. 57, no. 16, pp. 4258–4273, 2018.

[4] S. Kim, C. Laschi, and B. Trimmer, "Soft robotics: a bioinspired evolution in robotics," *Trends in biotechnology*, vol. 31, no. 5, pp. 287–294, 2013.

[5] J. Shintake, V. Cacucciolo, D. Floreano, and H. Shea, "Soft robotic grippers," *Advanced Materials*, p. 1707035, 2018.

[6] J. Hughes, U. Culha, F. Giardina, F. Guenther, A. Rosendo, and F. Iida, "Soft manipulators and grippers: a review," *Frontiers in Robotics and AI*, vol. 3, p. 69, 2016.

[7] M. R. Cutkosky, "On grasp choice, grasp models, and the design of hands for manufacturing tasks," *IEEE Transactions on robotics and automation*, vol. 5, no. 3, pp. 269–279, 1989.

[8] J. Shintake, S. Rosset, B. Schubert, D. Floreano, and H. Shea, "Versatile soft grippers with intrinsic electroadhesion based on multifunctional polymer actuators," *Advanced Materials*, vol. 28, no. 2, pp. 231–238, 2016.

[9] E. W. Schaler, D. Ruffatto, P. Glick, V. White, and A. Parness, "An electrostatic gripper for flexible objects," in *2017 IEEE/RSJ International Conference on Intelligent Robots and Systems (IROS)*. IEEE, 2017, pp. 1172–1179.

[10] D. Ruffatto, P. E. Glick, M. T. Tolley, and A. Parness, "Long-duration surface anchoring with a hybrid electrostatic and gecko-inspired adhesive," *IEEE Robotics and Automation Letters*, vol. 3, no. 4, pp. 4201–4208, 2018.

[11] A. Pettersson, S. Davis, J. Gray, T. Dodd, and T. Ohlsson, "Design of a magnetorheological robot gripper for handling of delicate food products with varying shapes," *Journal of Food Engineering*, vol. 98, no. 3, pp. 332–338, 2010.

[12] Y. T. Choi, C. M. Hartzell, T. Leps, and N. M. Wereley, "Gripping characteristics of an electromagnetically activated magnetorheological fluid-based gripper," *AIP Advances*, vol. 8, no. 5, p. 056701, 2018.

[13] L. U. Odhner, L. P. Jentoft, M. R. Claffee, N. Corson, Y. Tenzer, R. R. Ma, M. Buehler, R. Kohout, R. D. Howe, and A. M. Dollar, "A compliant, underactuated hand for robust manipulation," *The International Journal of Robotics Research*, vol. 33, no. 5, pp. 736–752, 2014.

[14] M. Manti, T. Hassan, G. Passetti, N. D'Elia, C. Laschi, and M. Cianchetti, "A bioinspired soft robotic gripper for adaptable and effective grasping," *Soft Robotics*, vol. 2, no. 3, pp. 107–116, 2015.

[15] Z. E. Teoh, B. T. Phillips, K. P. Becker, G. Whittredge, J. C. Weaver, C. Hoberman, D. F. Gruber, and R. J. Wood, "Rotary-actuated folding polyhedrons for midwater investigation of delicate marine organisms," *Science Robotics*, vol. 3, no. 20, p. eaat5276, 2018.

[16] L. Chin, J. Lipton, R. MacCurdy, J. Romanishin, C. Sharma, and D. Rus, "Compliant electric actuators based on handed shearing auxetics," in *2018 IEEE International Conference on Soft Robotics (RoboSoft)*. IEEE, 2018, pp. 100–107.

[17] J. I. Lipton, R. MacCurdy, Z. Manchester, L. Chin, D. Cellucci, and D. Rus, "Handedness in shearing auxetics creates rigid and compliant structures," *Science*, vol. 360, no. 6389, pp. 632–635, 2018.

[18] K. C. Galloway, K. P. Becker, B. Phillips, J. Kirby, S. Licht, D. Tchernov, R. J. Wood, and D. F. Gruber, "Soft robotic grippers for biological sampling on deep reefs," *Soft Robotics*, vol. 3, no. 1, pp. 23–33, 2016.

[19] B. S. Homberg, R. K. Katzschmann, M. R. Dogar, and D. Rus, "Haptic identification of objects using a modular soft robotic gripper," in *Intelligent Robots and Systems (IROS), 2015 IEEE/RSJ International Conference on*. IEEE, 2015, pp. 1698–1705.

[20] S. Terryn, J. Brancart, D. Lefeber, G. Van Assche, and B. Vanderborght, "Self-healing soft pneumatic robots," *Science Robotics*, vol. 2, no. 9, p. eaan4268, 2017.

[21] H. Zhao, J. Jalving, R. Huang, R. Knepper, A. Ruina, and R. Shepherd, "A helping hand: Soft orthosis with integrated optical strain sensors and emg control," *IEEE Robotics & Automation Magazine*, vol. 23, no. 3, pp. 55–64, 2016.

[22] R. Deimel and O. Brock, "A novel type of compliant and underactuated robotic hand for dexterous grasping," *The International Journal of Robotics Research*, vol. 35, no. 1-3, pp. 161–185, 2016.

[23] Y. Li, Y. Chen, Y. Yang, and Y. Wei, "Passive particle jamming and its stiffening of soft robotic grippers," *IEEE Transactions on Robotics*, vol. 33, no. 2, pp. 446–455, 2017.

[24] J. Zhou, S. Chen, and Z. Wang, "A soft-robotic gripper with enhanced object adaptation and grasping reliability," *IEEE Robotics and Automation Letters*, vol. 2, no. 4, pp. 2287–2293, 2017.

[25] Z. Wang, Y. Torigoe, and S. Hirai, "A prestressed soft gripper: design, modeling, fabrication, and tests for food handling," *IEEE Robotics and Automation Letters*, vol. 2, no. 4, pp. 1909–1916, 2017.

[26] E. Brown, N. Rodenberg, J. Amend, A. Mozeika, E. Steltz, M. R. Zakin, H. Lipson, and H. M. Jaeger, "Universal robotic gripper based on the jamming of granular material," *Proceedings of the National Academy of Sciences*, vol. 107, no. 44, pp. 18 809–18 814, 2010.

[27] J. R. Amend, E. Brown, N. Rodenberg, H. M. Jaeger, and H. Lipson, "A positive pressure universal gripper based on the jamming of granular material," *IEEE Transactions on Robotics*, vol. 28, no. 2, pp. 341–350, 2012.

[28] D. Yang, B. Mosadegh, A. Ainla, B. Lee, F. Khashai, Z. Suo, K. Bertoldi, and G. M. Whitesides, "Buckling of elastomeric beams enables actuation of soft machines," *Advanced Materials*, vol. 27, no. 41, pp. 6323–6327, 2015.

[29] D. Yang, M. S. Verma, J.-H. So, B. Mosadegh, C. Keplinger, B. Lee, F. Khashai, E. Lossner, Z. Suo, and G. M. Whitesides, "Buckling pneumatic linear actuators inspired by muscle," *Advanced Materials Technologies*, 2016.

[30] S. Li, D. M. Vogt, D. Rus, and R. J. Wood, "Fluid-driven origami-inspired artificial muscles," *Proceedings of the National Academy of Sciences*, p. 201713450, 2017.

[31] D.-Y. Lee, J.-S. Kim, J.-J. Park, S.-R. Kim, and K.-J. Cho, "Fabrication of origami wheel using pattern embedded fabric and its application to a deformable mobile robot," in *Robotics and Automation (ICRA), 2014 IEEE International Conference on*. IEEE, 2014, pp. 2565–2565.

[32] D.-Y. Lee, J.-S. Kim, S.-R. Kim, J.-S. Koh, and K.-J. Cho, "The deformable wheel robot using magic-ball origami structure," in *ASME 2013 international design engineering technical conferences and computers and information in engineering conference*. American Society of Mechanical Engineers, 2013, pp. V06BT07A040–V06BT07A040.

[33] P. H. Le, Z. Wang, and S. Hirai, "Origami structure toward floating aerial robot," in *Advanced Intelligent Mechatronics (AIM), 2015 IEEE International Conference on*. IEEE, 2015, pp. 1565–1569.

[34] H. Fang, Y. Zhang, and K. Wang, "An earthworm-like robot using origami-ball structures," in *Active and Passive Smart Structures and Integrated Systems 2017*, vol. 10164. International Society for Optics and Photonics, 2017, p. 1016414.

[35] B. H. Hanna, J. M. Lund, R. J. Lang, S. P. Magleby, and L. L. Howell, "Waterbomb base: a symmetric single-vertex bistable origami mechanism," *Smart Materials and Structures*, vol. 23, no. 9, p. 094009, 2014.

[36] Y. Chen, H. Feng, J. Ma, R. Peng, and Z. You, "Symmetric waterbomb origami," *Proc. R. Soc. A*, vol. 472, no. 2190, p. 20150846, 2016.

[37] S. Felton, M. Tolley, E. Demaine, D. Rus, and R. Wood, "A method for building self-folding machines," *Science*, vol. 345, no. 6197, pp. 644–646, 2014.

[38] M. T. Tolley, S. M. Felton, S. Miyashita, D. Aukes, D. Rus, and R. J. Wood, "Self-folding origami: shape memory composites activated by uniform heating," *Smart Materials and Structures*, vol. 23, no. 9, p. 094006, 2014.

[39] S. Miyashita, S. Guitron, S. Li, and D. Rus, "Robotic metamorphosis by origami exoskeletons," *Science Robotics*, vol. 2, no. 10, p. eaao4369, 2017.

[40] B. S. Homberg, R. K. Katzschmann, M. R. Dogar, and D. Rus, "Robust proprioceptive grasping with a soft robot hand," *Autonomous Robots*, pp. 1–16, 2018.

[41] R. L. Truby, M. Wehner, A. K. Grosskopf, D. M. Vogt, S. G. Uzel, R. J. Wood, and J. A. Lewis, "Soft somatosensitive actuators via embedded 3d printing," *Advanced Materials*, vol. 30, no. 15, p. 1706383, 2018.

[42] P. Glick, S. A. Suresh, D. Ruffatto, M. Cutkosky, M. T. Tolley, and A. Parness, "A soft robotic gripper with gecko-inspired adhesive," *IEEE Robotics and Automation Letters*, vol. 3, no. 2, pp. 903–910, 2018.

[43] C. Choi, W. Schwarting, J. DelPreto, and D. Rus, "Learning object grasping for soft robot hands," *IEEE Robotics and Automation Letters*, 2018.

[44] M. Pozzi, G. Salvietti, J. Bimbo, M. Malvezzi, and D. Prattichizzo, "The closure signature: a functional approach to model underactuated

compliant robotic hands," *IEEE Robotics and Automation Letters*, vol. 3, no. 3, pp. 2206–2213, 2018.